Macromolecules

Article

pubs.acs.org/Macromolecules

Synthesis and Properties of Multicleavable Amphiphilic Dendritic Comblike and Toothbrushlike Copolymers Comprising Alternating PEG and PCL Grafts

Meijing Zhang,† Huanhuan Liu,† Wei Shao, Ke Miao, and Youliang Zhao*

Jiangsu Key Laboratory of Advanced Functional Polymer Design and Application, Department of Polymer Science and Engineering, College of Chemistry, Chemical Engineering and Materials Science, Soochow University, Suzhou 215123, China

Supporting Information

ABSTRACT: Facile construction of novel functional dendritic copolymers by combination of self-condensing vinyl polymerization, sequence-controlled copolymerization and RAFT process was presented. RAFT copolymerization of a disulfide-linked polymerizable RAFT agent and equimolar feed ratio of styrenic and maleimidic macromonomers afforded multicleavable A_mB_n dendritic comblike copolymers with alternating PEG (A) and PCL (B) grafts, and a subsequent chain extension polymerization of styrene, *tert*-butyl acrylate, methyl methacrylate, and *N*-isopropylacrylamide gave $A_mB_nC_o$ dendritic toothbrushlike copolymers. $(PEG)_m(PCL)_n$ copolymers obtained were of adjustable molecular weight, relatively low polydispersity (PDI = 1.10−1.32), variable CTA functionality (f_{CTA} = 4.3−7.5), and similar segment numbers of PEG and PCL grafts, evident from ^{1}H NMR and GPC-MALLS analyses. Their branched architecture was confirmed by (a) reduction-triggered degradation, (b) decreased intrinsic viscosities and Mark−Houwink−Sakurada exponent than their "linear" analogue, and (c) lowered glass transition and melting temperatures and broadened melting range as compared with normal A_mB_n comblike copolymer. In vitro drug release results revealed that the drug release kinetics of the disulfide-linked A_mB_n copolymer aggregates was significantly affected by macromolecular architecture, end group and reductive stimulus. These stimuli-responsive and biodegradable dendritic copolymer aggregates had a great potential as controlled delivery vehicles.

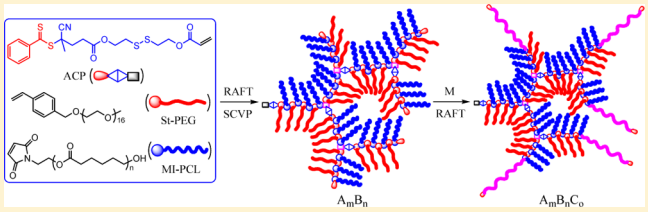

INTRODUCTION

Facile construction of complex macromolecular architectures such as dendritic and hyperbranched copolymers,[1−10] star polymers[11−21] and polymer brushes[22−30] have attracted much attention due to their unique physicochemical properties and multipurpose applications originating from the branched topologies. As a subclass of dendritic polymers, segmented hyperbranched copolymers comprising long linear branched chains are of increasing interest due to their wide chemical composition, adjustable degree of branching and chain length, and ability for versatile postfunctionalization. Generally speaking, self-condensing vinyl polymerization (SCVP)[31] via controlled radical processes such as atom transfer radical polymerization (ATRP)[32−36] and reversible addition−fragmentation chain transfer (RAFT) polymerization[37−43] can be efficiently used to achieve hyperbranched architectures with variable molecular parameters. RAFT SCVP was previously used by us to achieve hyperbranched copolymers with variable chain transfer agent (CTA) functionality and relatively low polydispersity, and a variety of multiarm and miktoarm star polymers with a branched core were further generated by subsequent chain extension polymerization and/or quaternization reaction between branched scaffolds and bromide-functionalized polymers.[41,42] More recently, Gao and coworkers ingeniously combined RAFT SCVP, Menschutkin reaction and Cu(I) catalyzed azide−alkyne cycloaddition reaction to synthesize hyperbranched macroinitiators, dendritic polymer brushes, and star-shaped polymers.[43] With the development in advanced polymer synthesis, it is extremely urgent to further apply hyperbranched copolymers as versatile scaffolds to construct novel dendritic and starlike copolymers via postmodification and postpolymerization in addition to pursuing for ideal approaches to rapid synthesis of the target copolymers.

Meanwhile, much emphasis has been paid to sequence-regulated polymerization since the introduction of regular microstructures involving alternating AB, AAB, and ABA sequences into well-defined copolymers usually endows functional materials with new features such as novel self-assembled nanoobjects, unique degradation and crystallization behaviors and tunable amphiphilic properties.[44−67] To date, a series of copolymers comprising precise microstructures have been successfully achieved by chain growth polymerization. Among them, maleimidic and styrenic monomers are generally liable to alternating copolymerization, and thus numerous alternating and sequence-controlled copolymers,[52−57] copolymer brushes,[58−62] and dendritic-linear block copolymers with alternating AB sequences[63−65] have been precisely prepared by

Received: December 9, 2012
Revised: January 31, 2013
Published: February 11, 2013

dx.doi.org/10.1021/ma3025283 | Macromolecules 2013, 46, 1325−1336

Scheme 1. Synthetic Routes to Multicleavable Amphiphilic A_mB_n-Type Dendritic Comblike Copolymers and $A_mB_nC_o$-Type Dendritic Toothbrushlike Copolymers

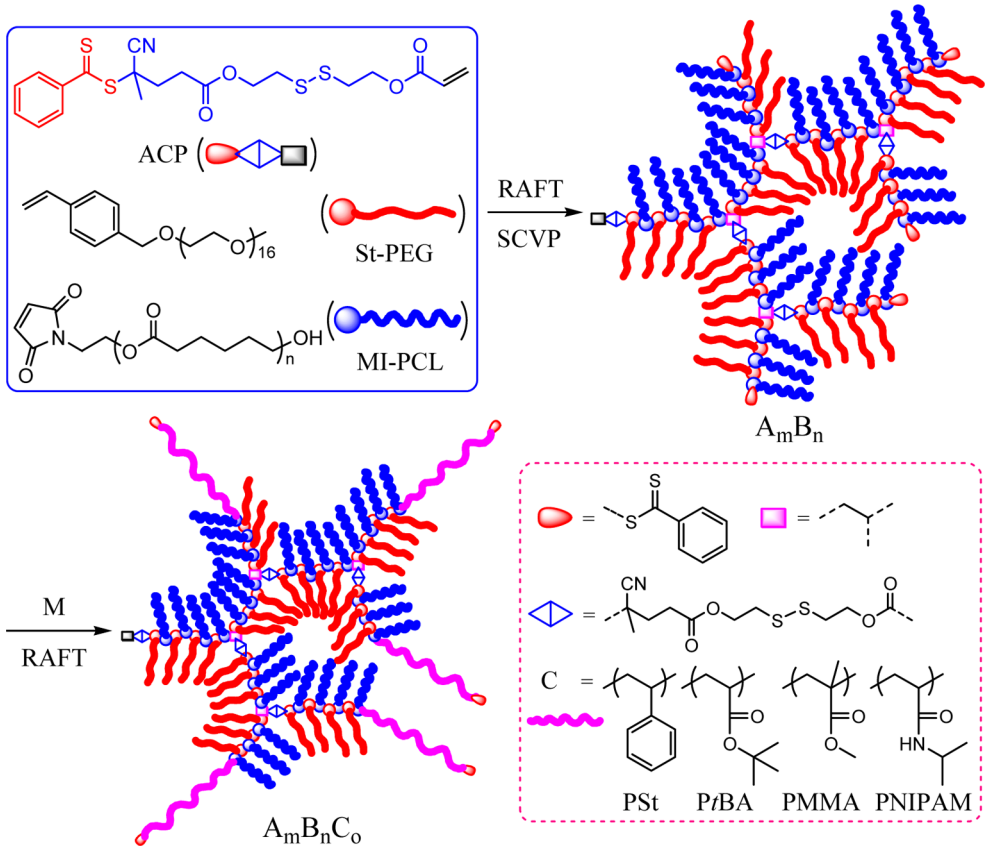

radical copolymerization. Chen and co-workers previously reported both (a) atom transfer radical copolymerization of maleimidic inimer with St and (b) controlled radical copolymerization of bismaleimide with excess St could generate multiarm PSt stars via one-pot process, revealing the great potential of alternating copolymerization in novel architecture construction.[66,67] We used RAFT copolymerization of vinylbenzyl-terminated PEG (St-PEG) and *N*-(2-hydroxyethyl) maleimide (HEMI) to synthesize well-defined symmetric disulfide-linked $A_{2m}B_{2n}$-type comblike copolymers[62] and $A_{2m}B_{2n}C_2$-type starlike terpolymers[20] with alternating poly(ethylene glycol) (PEG, A) and poly(ε-caprolactone) (PCL, B) pendent chains. These copolymers could be efficiently converted into degraded thiol-terminated comblike and starlike copolymers upon reduction, and followed by oxidation to form disulfide-linked high-molecular-weight copolymer brushes and comblike-linear multiblock copolymers; such redox cycles could be efficiently repeated.[20,62] To our surprise, the examples of hyperbranched and dendritic copolymers with regular sequences are very scarce thus far.[68,69] Only a few hyperbranched alternating block copolymers were prepared by Perrier and coworkers via thiol−yne "click" chemistry, in which RAFT synthesized clickable diblock copolymers were used as precursors to linear branches.[68,69] At present, accelerated construction of new functional copolymers via sequence-controlled polymerization is of great importance since it not only introduces intriguing phase morphologies and multiple stimuli-responsive properties but has promising applications in smart biomaterials and nanotechnologies.

Herein, we report on facile synthesis of novel multicleavable amphiphilic dendritic comblike and toothbrushlike copolymers with alternating PEG and PCL grafts by combination of self-condensing vinyl polymerization, sequence-controlled copolymerization and RAFT process (Scheme 1). RAFT copolymerization of styrenic and maleimidic macromonomers mediated by 2-((2-(acryloyloxy)ethyl)disulfanyl)ethyl 4-cyano-4-(phenylcarbonothioylthio)pentanoate (ACP) afforded A_mB_n-type dendritic comblike copolymers with alternating PEG (A) and PCL (B) grafts in each branch and cleavable disulfide moiety in each branching point, and $A_mB_nC_o$-type dendritic toothbrushlike copolymers were further generated by A_mB_n copolymer mediated chain extension polymerization. The resultant dendritic copolymers were characterized by ^{1}H NMR, GPC-MALLS, DSC and viscosity measurement. Meanwhile, stimuli-triggered drug loading and release from the self-assembled A_mB_n copolymer aggregates were preliminarily investigated. To the best of our knowledge, this is the first example on facile synthesis of dendritic comblike copolymers with high-density alternating grafts on the basis of sequence-controlled copolymerization. The methodology developed in this study has a great potential in accelerated construction of versatile thiol-responsive A_mB_n and $A_mB_nC_o$ ($m \approx n$) dendritic copolymers with rich chemical composition, tunable dithiobenzoate and disulfide functionalities, and variable number and chain length of C segments. In addition, the presence of terminal hydroxyl functionalities in PCL segments allows for chain extension polymerization and versatile postmodification to introduce different varieties of polymer segments and functionalities.

dx.doi.org/10.1021/ma3025283 | *Macromolecules* 2013, 46, 1325−1336

Table 1. Synthesis of A_mB_n Dendritic Comblike Copolymers (DC1-DC8) and Normal Comblike Copolymer (C1) by RAFT Copolymerization of St-PEG and MI-PCL Mediated by ACP (Runs 1-8) and CPDB (Run 9)[a]

run	sample	DP_{PCL}	x	C_{CTA} (%)[b]	C%[b]	$M_{n,LS}$[c]	PDI[c]	$[\eta]_w$ (mL/g)[d]	f_{CTA}[e]	m[f]	n[f]
1	DC1	8.2	5	93.3	56.8	46 600	1.32	13.5	7.5	22.5	21.8
2	DC2	8.2	20	95.8	35.2	78 300	1.10	15.1	5.4	39.2	38.6
3	DC3	8.2	20	99.5	50.8	136 000	1.21	17.6	7.0	68.6	67.2
4	DC4	12.6	5	54.6	39.2	62 000	1.20	9.2	6.8	24.5	23.8
5	DC5	12.6	10	25.9	35.1	148 600	1.19	13.6	4.3	59.8	61.1
6	DC6	12.6	20	19.6	28.5	312 000	1.20	15.2	4.3	125	126
7	DC7	43.2	1	29.4	35.2	52 100	1.23	20.1	6.8	8.5	8.2
8	DC8	43.2	5	51.1	30.3	89 500	1.28	26.5	5.0	14.9	14.6
9	C1	8.2	20	99.7	53.9	22 500	1.22	11.6	0.96	11.5	11.2

[a]Polymerization conditions: $[St\text{-}PEG]_0:[MI\text{-}PCL]_0:[CTA]_0:[AIBN]_0 = x:x:1:0.2$, $[MI\text{-}PCL]_0 = 0.20$ (runs 1−3 and 9) or 0.05 mol/L (runs 4−8), in dioxane at 80 °C for 48 (runs 3 and 9) or 24 h (other runs). [b]Total monomer conversion (C) and ACP conversion (C_{CTA}) determined by combination of gravimetry and ^{1}H NMR analysis. [c]Number-average molecular weight and polydispersity determined by GPC−MALLS. [d]Weight-average intrinsic viscosity. [e]Number-average CTA functionality per copolymer. [f]Number-average segment numbers of PEG (m) and PCL (n) grafts per copolymer.

EXPERIMENTAL SECTION

Materials. All solvents, monomers, and other chemicals were purchased from Sigma-Aldrich unless otherwise stated. ε-Caprolactone (CL, 99%) and bis(2-hydroxyethyl) disulfide (Alfa Aesar, 90%) were distilled from calcium hydride under reduced pressure. Styrene (St, 99%), 4-vinylbenzyl chloride (VBC, 90%), methyl methacrylate (MMA, 99%) and *tert*-butyl acrylate (*t*BA, 98%) were passed through a basic alumina column to remove the inhibitor before use. *N*-Isopropylacrylamide (NIPAM, 97%) was recrystallized twice from mixtures of hexane and toluene. 2,2′-Azobis(isobutyronitrile) (AIBN) was recrystallized twice from ethanol. Monomethoxy poly(ethylene glycol) (MPEG, M_n = 750, Fluka) was dried by azeotropic distillation in the presence of toluene. Vinylbenzyl-terminated PEG (St-PEG),[59] 4-(2-hydroxyethyl)-10-oxa-4-aza-tricyclo[5.2.1.02,6]dec-8-ene-3,5-dione (HTD),[70] 2-(2-cyanopropyl) dithiobenzoate (CPDB),[37] 4-cyanopentanoic acid dithiobenzoate (4-CPDB),[71] and 2-((2-hydroxyethyl)disulfanyl)ethyl 4-cyano-4-(phenylcarbonothioylthio)-pentanoate[72] were synthesized and purified according to literature procedures. *N*,*N*′-Dicyclohexylcarbodiimide (DCC) and 4-dimethylaminopyridine (DMAP) were purchased from Sinopharm Chemical Reagent Co., Ltd. and used as received. D,L-Dithiothreitol (DTT, 99%, Merck) and doxorubicin hydrochloride (>99%, Zhejiang Hisun Pharmaceutical Co, Ltd.) were used as received. Dichloromethane (DCM) and dioxane were dried and distilled over CaH_2. Tetrahydrofuran (THF) and toluene were distilled over sodium and benzophenone and stored under nitrogen.

Synthesis of 2-((2-(Acryloyloxy)ethyl)disulfanyl)ethyl 4-Cyano-4-(Phenylcarbonothioylthio) pentanoate (ACP). To a 250 mL of round flask were added 2-((2-hydroxyethyl)disulfanyl)ethyl 4-cyano-4-(phenylcarbonothioylthio)pentanoate (2.49 g, 6.0 mmol), acrylic acid (0.50 g, 6.9 mmol), DMAP (0.12 g, 1.0 mmol) and 100 mL of dry DCM under nitrogen, and followed by slow addition of a 30 mL of DCM solution with 1.55 g (7.5 mmol) of DCC to perform the esterification. The mixture was further stirred at ambient temperature overnight. The crude product was filtered, concentrated and purified by flash column chromatography eluting with hexane/DCM (2:1), and 2.26 g (80.2% yield) of ACP was obtained as a red oil.

^{1}H NMR (300 MHz, $CDCl_3$): δ 7.92 (d, J 7.5, Ph*H*, 2H), 7.56 (t, J 6.9, Ph*H*, 1H), 7.39 (t, J 7.5, Ph*H*, 2H), 6.46, 6.14, and 5.87 (m, C*H*═CH_2, 3H), 4.41 and 4.38 (m, CH_2O, 4H), 2.96 (dd, J 6.9, CH_2S, 4H), 2.70, 2.62, and 2.45 (m, CH_2CH_2CO, 4H), 1.93 (s, CH_3, 3H). ^{13}C NMR (75 MHz, $CDCl_3$): δ 222.1 (*C*═S), 171.1, 165.7 (C═O), 144.3, 133.0, 131.3, 128.5, 127.9, 126.5 (Ph*C* and *C*H═CH_2), 118.3 (*C*N), 62.6, 62.2 (CH_2O), 45.6 (CH_3CCN), 37.0, 36.9 (CH_2S), 33.1, 29.6 (CH_2), 24.0 (CH_3). FT-IR (KBr): 3262, 3060, 2934, 2853, 2231, 1732, 1649, 1635, 1618, 1590, 1543, 1445, 1407, 1296, 1268, 1181, 1109, 1079, 1049, 983, 902, 868, 810, 763, 688, 650, 617 cm^{-1}. Anal. Calcd for $C_{20}H_{23}NO_4S_4$: C, 51.15; H, 4.94; N, 2.98; S, 27.31. Found: C, 51.32; H, 4.96; N, 2.95; S, 27.09.

Synthesis of MI-PCL Macromonomers. In a typical reaction (run 1 of Table S1, Supporting Information), to a Schlenk tube were added HTD (1.05 g, 5.0 mmol), CL (11.4 g, 100 mmol), $Sn(Oct)_2$ (0.203 g, 0.50 mmol), and 22 mL of dry toluene under nitrogen. The contents were stirred for 5 min and subjected to three freeze-vacuum-thaw cycles, and then the tube was immersed into an oil bath at 110 °C to perform polymerization. After 20 h, the polymerization was quenched by putting the tube into an ice−water bath. About 0.1 mL of polymerization solution was drawn to check ^{1}H NMR spectroscopy, and monomer conversion was determined to be 79.2% by ^{1}H NMR analysis. The polymerization solution was concentrated and precipitated into a large amount of cold hexane. The isolated PCL was dissolved in 100 mL of anisole, and the solution was heated at 120 °C for 16 h. After concentration and precipitation, 9.2 g of MI-PCL was obtained. The apparent molecular weight and polydispersity estimated by GPC were $M_{n,GPC}$ = 1990 and PDI = 1.10. The number-average molecular weight determined by ^{1}H NMR was $M_{n,NMR}$ = 1080, which was close to theoretical value ($M_{n,th}$ = 1040). Other MI-PCL samples were synthesized and purified according to similar procedures. ^{1}H NMR ($CDCl_3$): δ 6.76 (C*H*═C*H*), 4.24 (NCH_2CH_2O), 4.06 (CH_2O of PCL), 3.80 (CH_2N), 3.66 (CH_2OH), 2.31 (CH_2CO of PCL), 1.65 and 1.40 (CH_2CH_2CH_2CH_2O of PCL). ^{13}C NMR ($CDCl_3$): δ 173.40 (*C*═O), 170.28 (*C*═O of MI ring), 134.12 (CH═*C*H), 63.98 (CH_2O of CL unit), 62.22 (CH_2OH), 61.17 (NCH_2CH_2O), 36.77 (NCH_2), 33.95 (CH_2CO of CL unit), 33.62 (CH_2CO of terminal CL unit), 32.15 (CH_2CH_2OH), 28.16 (CH_2CH_2O of CL unit), 25.36 (CH_2CH_2CH_2O of CL unit), 25.18 (CH_2CH_2CH_2CH_2OH), 24.55 (CH_2CH_2CH_2OH), 24.41 (CH_2CH_2CO of CL unit). FT-IR (KBr): 3437, 2945, 2864, 1724, 1471, 1420, 1398, 1369, 1296, 1247, 1195, 1106, 1047, 963, 934, 839, 732, 697 cm^{-1}.

Synthesis of A_mB_n Dendritic Comblike Copolymers by RAFT Self-Condensing Vinyl Copolymerization. In a typical experiment (run 2 of Table 1), ACP (94.0 mg, 0.20 mmol), St-PEG (3.48 g, 4.0 mmol), MI-PCL (4.32 g, 4.0 mmol), and AIBN (6.6 mg, 0.04 mmol) were added to a Schlenk tube, and dry dioxane was added until the total volume was 20.0 mL. The contents were degassed with bubbled nitrogen for 30 min, and then the polymerization was performed at 80 °C for 24 h. The polymerization solution was precipitated into diethyl ether thrice, and 2.84 g (35.2% total monomer conversion) of $(PEG)_m(PCL)_n$ copolymer (denoted as DC2) was obtained after vacuum drying. The conversion of ACP (C_{CTA}) was determined to be 95.8% by combination of gravimetry and ^{1}H NMR analysis. Number-average molecular weight and polydispersity determined by GPC-MALLS were $M_{n,LS}$ = 78300 and PDI = 1.10. Based on GPC-MALLS and NMR analyses, its number-average CTA functionality (f_{CTA}) was determined to be 5.4, and number-average segment number of each graft was calculated to be m_{PEG} = 39.2, and n_{PCL} = 38.6. Other dendritic comblike copolymers were synthesized and isolated

dx.doi.org/10.1021/ma3025283 | *Macromolecules* 2013, 46, 1325−1336

Table 2. Synthesis of $A_mB_nC_o$ (A = PEG, B = PCL, C = PM) Dendritic Toothbrushlike Copolymers by RAFT Polymerization Mediated by DC2 ($M_{n,LS}$ = 78300, f_{CTA} = 5.4)[a]

run	M	DP_0	C %[b]	$M_{n,th}$[c]	$M_{n,LS}$[d]	PDI[d]	$M_{n,NMR}$[e]	dn/dc[f]	$[\eta]_w$ (mL/g)[g]
1	St	200	19.9	100 700	105 100	1.06	103 200	0.104	19.4
2	*t*BA	150	46.8	126 900	125 700	1.09	128 000	0.0758	25.1
3	MMA	150	38.6	109 600	109 300	1.11	107 800	0.0857	20.2
4	NIPAM	150	47.2	121 500	121 400	1.13	122 600	0.0886	23.9

[a]Polymerization conditions: $[M]_0$:($f_{CTA}[\text{macro CTA}]_0$):$[AIBN]_0$ = DP_0:1:0.2, $[M]_0$ = 1.5 mol/L, in toluene (runs 1−3) or dioxane (run 4) at 80 °C for 12 h. [b]Monomer conversion determined by gravimetry. [c]Theoretical molecular weight, $M_{n,th}$ = 78300 + f_{CTA} × DP_0 × conversion × MW_M, in which MW_M was molecular weight of vinyl monomers. [d]Number-average molecular weight and polydispersity determined by GPC-MALLS. [e]Number-average molecular weight determined by ^{1}H NMR. [f]Determined by refractive index detector. [g]Weight-average intrinsic viscosity.

according to a similar approach. Besides, a normal A_mB_n comblike copolymer (denoted as C1) was also prepared by RAFT copolymerization of St-PEG and MI-PCL mediated by CPDB.

(PEG)$_m$(PCL)$_n$ Dendritic Comblike Copolymer. ^{1}H NMR ($CDCl_3$): δ 7.98 (Ph*H* of terminal PhC(=S)S), 6.2−7.8 (Ar*H* of St-PEG unit and Ph*H* of terminal PhC(=S)S), 4.8−5.1 (CHS), 4.50 and 4.24 (CH_2O), 4.06 (CH_2O of PCL), 3.87 (C*H* of MI-PCL unit), 3.65 (CH_2CH_2O of PEG), 3.56 (CH_2N of MI-PCL unit), 3.38 (CH_3O of PEG), 0.8−3.0 (C*H*, CH_2 and CH_3 originating from RAFT agent, maleimidic and styrenic units). FT-IR (KBr): 3464, 2939, 2867, 1728, 1702, 1638, 1466, 1398, 1352, 1296, 1246, 1193, 1105, 1041, 953, 849, 733, 669 cm^{-1}.

Degradation and Aminolysis of Dendritic Comblike Copolymers. Dried DC2 copolymer (30 mg) was dissolved in 3.0 mL of THF under nitrogen, and about 2.0 μL of Bu_3P was added to the solution at ambient temperature. The mixture was stirred overnight, diluted with THF and subjected to GPC analysis. Molecular weight and polydispersity of degraded $(PEG)_x(PCL)_y$ comblike copolymer were $M_{n,LS}$ = 17900, PDI = 1.36.

Aminolysis was used to prepare multithiol-functionalized $(PEG)_m(PCL)_n(SH)_o$ copolymer. Under nitrogen, 0.50 g of DC2 copolymer was dissolved in 10 mL of THF, and followed by slow addition of a solution of 10-fold excess of hydrazine in THF. After stirring for 2 h, the mixture was concentrated and precipitated, and DC2-SH copolymer was isolated as white powders. $M_{n,LS}$ = 79600, PDI = 1.12.

Synthesis of $A_mB_nC_o$ Dendritic Toothbrushlike Copolymers by Chain Extension Polymerization. In a typical polymerization (run 1 of Table 2), DC2 copolymer (0.50 g, 34.5 μmol CTA), St (0.72 g, 6.9 mmol), AIBN (1.1 mg, 6.7 μmol) were added to a Schlenk tube, and toluene was added until the total volume was 4.6 mL. After degassing with bubbled nitrogen for 20 min, the mixture was polymerized at 80 °C for 12 h. The polymerization solution was precipitated into methanol thrice, and 0.643 g (19.9% conversion) of $(PEG)_m(PCL)_n(PSt)_o$ copolymer was isolated. $M_{n,LS}$ = 105100, PDI = 1.06. Other dendritic toothbrushlike copolymers were synthesized and purified according to similar procedures.

(PEG)$_m$(PCL)$_n$(PSt)$_o$ Copolymer. ^{1}H NMR ($CDCl_3$): δ 7.86 (Ph*H* of terminal PhC(=S)S), 6.2−7.7 (Ph*H* of PSt, Ar*H* of St-PEG unit and Ph*H* of terminal PhC(=S)S), 4.6−5.1 (CHS), 4.50 and 4.30 (CH_2O), 4.06 (CH_2O of PCL), 3.88 (C*H* of MI-PCL unit), 3.65 (CH_2CH_2O of PEG and CH_2N of MI-PCL unit), 3.38 (CH_3O of PEG), 0.8−3.0 (C*H*, CH_2 and CH_3 originating from RAFT agent, maleimidic and styrenic units). FT-IR (KBr): 3447, 3081, 3059, 3025, 2923, 2868, 1774, 1737, 1701, 1602, 1560, 1493, 1454, 1398, 1352, 1299, 1280, 1251, 1146, 1105, 1031, 952, 848, 758, 700 cm^{-1}.

(PEG)$_m$(PCL)$_n$(PtBA)$_o$ Copolymer. ^{1}H NMR ($CDCl_3$): δ 7.90 (Ph*H* of terminal PhC(=S)S), 6.2−7.7 (Ar*H* of St-PEG unit and Ph*H* of terminal PhC(=S)S), 4.64 (CHS), 4.50 and 4.30 (CH_2O), 4.06 (CH_2O of PCL), 3.88 (C*H* of MI-PCL unit), 3.65 (CH_2CH_2O of PEG and CH_2N of MI-PCL unit), 3.38 (CH_3O of PEG), 0.8−3.0 (C*H*, CH_2 and CH_3 originating from RAFT agent, maleimidic and styrenic units, and *t*BA unit). FT-IR (KBr): 3435, 2933, 2868, 1731, 1705, 1638, 1561, 1459, 1394, 1368, 1350, 1256, 1154, 1100, 1036, 953, 846, 751 cm^{-1}.

(PEG)$_m$(PCL)$_n$(PMMA)$_o$ Copolymer. ^{1}H NMR ($CDCl_3$): δ 7.96 (Ph*H* of terminal PhC(=S)S), 6.2−7.7 (Ar*H* of St-PEG unit and Ph*H* of terminal PhC(=S)S), 4.50 and 4.30 (CH_2O), 4.06 (CH_2O of PCL), 3.88 (C*H* of MI-PCL unit), 3.65 (CH_2CH_2O of PEG), 3.60 (CH_3O of PMMA and CH_2N of MI-PCL unit), 3.38 (CH_3O of PEG), 0.8−3.0 (C*H*, CH_2 and CH_3 originating from RAFT agent, maleimidic and styrenic units, and MMA unit). FT-IR (KBr): 3448, 2946, 2870, 1732, 1703, 1638, 1560, 1459, 1398, 1352, 1275, 1245, 1194, 1152, 1099, 1038, 991, 954, 845, 749 cm^{-1}.

(PEG)$_m$(PCL)$_n$(PNIPAM)$_o$ Copolymer. ^{1}H NMR ($CDCl_3$): δ 7.90 (Ph*H* of terminal PhC(=S)S), 6.2−7.7 (Ar*H* of St-PEG unit and Ph*H* of terminal PhC(=S)S), 4.59 (CHS), 4.50 and 4.30 (CH_2O), 4.06 (CH_2O of PCL), 4.01 (C*H* of PNIPAM), 3.88 (C*H* of MI-PCL unit), 3.65 (CH_2CH_2O of PEG and CH_2N of MI-PCL unit), 3.38 (CH_3O of PEG), 0.8−3.0 (C*H*, CH_2 and CH_3 originating from RAFT agent, maleimidic and styrenic units, and NIPAM unit). FT-IR (KBr): 3439, 3293, 3072, 2932, 2871, 1736, 1704, 1647, 1545, 1459, 1389, 1364, 1352, 1279, 1251, 1171, 1101, 1037, 953, 847 cm^{-1}.

Self-Assembly and In Vitro Drug Release from A_mB_n Copolymer Aggregates. The copolymer aggregates were prepared by dialysis method. A_mB_n copolymer (5.0 mg) was dissolved in 1.0 mL of DMSO at room temperature, and then the polymer solution was added dropwise into 9.0 mL of phosphate buffered saline (PBS, pH 7.4, 50 mM) solution under vigorous stirring. Two hours later, the solution was transferred into dialysis membrane tubing (MWCO 3500) and dialyzed against PBS solution for 50 h to completely remove the organic solvent. The solution of copolymer aggregates was stored at 4 °C before measurement, and the size and morphology of aggregates were determined by DLS and TEM, respectively.

A similar procedure was used to prepare doxorubicin (DOX)-loaded aggregates. In a typical run, A_mB_n copolymer (10.0 mg) and DOX hydrochloride (2.0 mg) were dissolved in 1.0 mL of DMSO, and followed by addition of about 0.6 mg of triethylamine. The mixed solution was added dropwise to 19.0 mL of PBS solution (pH 7.4, 50 mM). After stirring for an additional 4 h, the solution was dialyzed against PBS solution for 50 h (MWCO 3500). The amount of DOX was determined using fluorescence (FLS920) measurement (excitation at 480 nm and emission at 560 nm). The drug loading capacity (DLC) and drug loading efficiency (DLE) of aggregates were determined by fluorescence analysis. In a typical run for drug release, two portions of DOX-loaded copolymer aggregates in PBS solution (4.0 mL, pH 7.4) were put into a dialysis bag (MWCO 5000), which were then immersed into 20 mL of (a) PBS solution (50 mM, pH 7.4) with 10 mM DTT or (b) normal PBS solution (50 mM, pH 7.4) at 37 °C. At predetermined time intervals, the drug-release solution was changed, and the amount of DOX released from aggregates was measured by fluorescence measurement (excitation at 480 nm) at room temperature. All release experiments were performed in triplicate.

Characterization. Apparent number-average molecular weight ($M_{n,GPC}$) and polydispersity (PDI) of St-PEG and MI-PCL macromonomers were measured on a Waters 150-C GPC using three Ultrastyragel columns (pore size 50, 100, and 1000 nm) with 10 μm bead size at 35 °C. THF was used as an eluent at a flow rate of 1.0 mL/min, and samples were calibrated using PMMA standard samples. Gel permeation chromatography with multiple angle laser scattering detection (GPC-MALLS) systems was used to determine absolute

dx.doi.org/10.1021/ma3025283 | *Macromolecules* 2013, 46, 1325−1336

number-average molecular weight ($M_{n,LS}$), polydispersity and solution viscosity of various copolymers. GPC was conducted in THF at 35 °C with a flow rate of 1.0 mL/min. Three TSK-GEL H-type columns (pore size 15, 30, and 200 Å, with molecular weight range of 100−1000, 300−20000, and 5000−400000 g/mol, respectively) with 5 μm bead size were used. Detection consisted of a RI detector (Optilab rEX), a multiangle (14−145°) laser light scattering (MALLS) detector (DAWN HELEOS) with the He−Ne light wavelength at 658.0 nm, and online viscosity detector (ViscoStar). The refractive index increment dn/dc for samples were measured off-line by Optilab rEX refractive index detector (λ = 658 nm) at 25 °C using a series of different concentration solutions. Data were collected and processed by use of ASTRA software from Wyatt Technology, and molecular weights were determined by the triple detection method. The intrinsic viscosity of copolymer solutions in THF was measured using a viscosimetric detector connected to GPC system at 35 °C. ^{1}H and ^{13}C NMR spectra were recorded on a Varian spectrometer at 25 °C using $CDCl_3$ as a solvent. Fourier transform infrared (FT-IR) spectra were recorded on a Perkin-Elmer 2000 spectrometer using KBr disks. C, H, N, and S were determined by combustion followed by chromatographic separation and thermal conductivity detection using a Carlo-Erba EA 1110CHNO-S elemental analyzer. Differential scanning calorimetry (DSC) analysis was performed under nitrogen atmosphere using a SDT 2960 Simultaneous DSC−TGA of TA Instruments with heating rate of 10 °C/min. Dynamic light scattering (DLS) measurements were carried out at 25 °C using Zetasizer Nano-ZS from Malvern Instruments equipped with a 633 nm He−Ne laser using backscattering detection, and the micellar solutions were filtered through a 450 nm syringe filter before measurements. Fluorescence spectroscopy was recorded at 25 °C on a FLS920 fluorescence spectrometer. Transmission electron microscopy (TEM) images were obtained through a Hitachi H-600 electron microscope.

RESULTS AND DISCUSSION

This study aimed at versatile synthesis and properties of disulfide-functionalized dendritic comblike and toothbrushlike copolymers. St-PEG and MI-PCL, as monomer pairs with strong tendency for alternating copolymerization, were subjected to RAFT copolymerization in the presence of ACP to form A_mB_n-type dendritic comblike copolymers, and $A_mB_nC_o$-type dendritic toothbrushlike copolymers were generated by a subsequent chain extension polymerization. The resultant copolymers were characterized by ^{1}H NMR, GPC-MALLS, DSC, and viscosity measurement, and DOX-loading and release properties of typical A_mB_n copolymers were investigated as well.

Synthesis of MI-PCL Macromonomers. MI-PCL was synthesized by two step reactions involving (a) ROP of CL initiated with 4-(2-hydroxyethyl)-10-oxa-4-aza-tricyclo-[5.2.1.02,6]dec-8-ene-3,5-dione (HTD) and (b) a subsequent deprotection at 120 °C to release the maleimide ring (Table S1, Supporting Information). In ^{1}H NMR spectra (Figure 1), characteristic signals of terminal group were noted at δ 6.76 (C*H*=C*H*), 4.24 (NCH$_2$C*H*$_2$O), 3.80 (C*H*$_2$N) and 3.66 (terminal C*H*$_2$OH), and signals of C*H*$_2$ in PCL segment appeared at δ 4.06 (C*H*$_2$O), 2.31 (C*H*$_2$CO), 1.65 and 1.40 (C*H*$_2$CH$_2$C*H*$_2$CH$_2$O). The polymerization degree (DP) of MI-PCL could be determined by equation $DP_{NMR} = I_{2.31}/I_{6.76}$ where I meant the integrated peak area. The molecular weights determined by ^{1}H NMR ($M_{n,NMR}$) were in the range of 1080−5070, which agreed well with the expected values ($M_{n,th}$). The GPC traces exhibited monomodal distribution with polydispersity in the range of 1.10−1.18 (Figure 2). These results revealed the two-step strategy could afford the target MI-PCL macromonomers with well-controlled molecular weight.

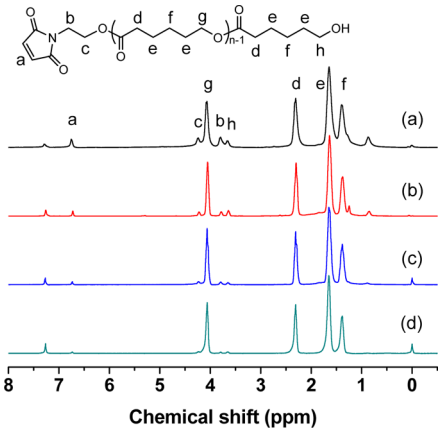

Figure 1. ^{1}H NMR spectra of MI-PCL macromonomers synthesized by runs 1−4 of Table S1, Supporting Information.

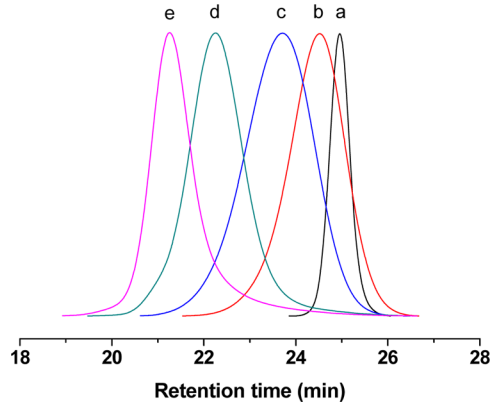

Figure 2. GPC traces of St-PEG (a) and MI-PCL (b−e) macromonomers. Apparent M_n and PDI values: 1570, 1.04 (a); 1990, 1.10 (b); 2920, 1.13 (c); 5260, 1.14 (d); 8090, 1.18 (e).

Synthesis of Dendritic Comblike Copolymers by RAFT SCVP. RAFT copolymerization in the presence of a polymerizable RAFT agent allows for one-pot synthesis of segmented hyperbranched copolymers with variable degree of branching and CTA functionality (f_{CTA}).[41−43] A disulfide-linked RAFT agent 2-((2-(acryloyloxy)ethyl)disulfanyl)ethyl 4-cyano-4-(phenylcarbonothioylthio)pentanoate (ACP) was first synthesized by esterification between 2-((2-hydroxyethyl)disulfanyl)-ethyl 4-cyano-4-(phenylcarbonothioylthio)pentanoate and acrylic acid, which acted as a versatile core reagent to generate multicleavable dendritic comblike copolymers. Unlike normal segmented hyperbranched copolymers with long linear branches,[38−43] the dendritic comblike copolymers obtained herein had branches composed of comblike copolymers with alternating PEG and PCL grafts and multiple disulfide functionalities in branching points, which enabled versatile topological transformations via postpolymerization and post-modification.

ACP and equimolar feed ratio of St-PEG ($M_{n,NMR}$ = 870, PDI = 1.04) and MI-PCL ($M_{n,NMR}$ = 1080, 1580 or 5070) macromonomers were subjected to RAFT SCVP to generate disulfide-functionalized A_mB_n dendritic comblike copolymers (DC1-DC8 of Table 1). In ^{1}H NMR spectra of typical A_mB_n copolymers (Figure 3), the characteristic signals of aromatic protons originating from ACP were noted at δ 7.98 (2H of Ph*H*, terminal PhC(=S)S) and 6.2−7.8 (Ar*H* and other Ph*H*),

dx.doi.org/10.1021/ma3025283 | Macromolecules 2013, 46, 1325−1336

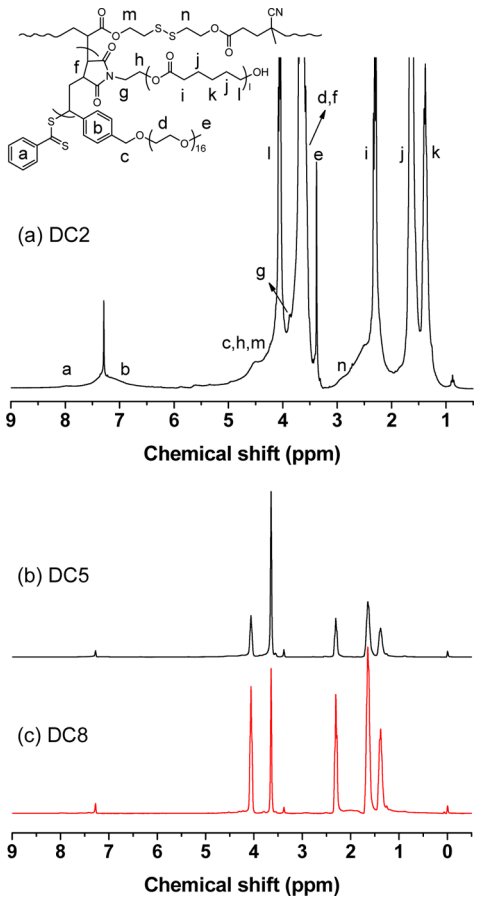

Figure 3. ^{1}H NMR spectra of typical A_mB_n dendritic comblike copolymers.

the signals of CH_2 protons in PCL segment appeared at δ about 4.06, 2.31, 1.65 and 1.40, and the signals in PEG segment appeared at δ 3.65 (CH_2CH_2O) and 3.38 (CH_3O). Therefore, number-average dithiobenzoate functionality could be calculated by equation $f_{CTA} = M_{n,LS} \times I_{7.98}/(MW_{CTA} \times I_{7.98} + M_{n,NMR}(St\text{-}PEG) \times I_{3.65}/(2DP_{PEG}) + M_{n,NMR}(MI\text{-}PCL) \times I_{4.06}/(DP_{PCL} - 1))$, and number-average segment numbers of PEG (m) and PCL (n) grafts per copolymer could be deduced by equations $m = f_{CTA} \times I_{3.65}/(2DP_{PEG} \times I_{7.98})$, and $n = f_{CTA} \times I_{4.06}/((DP_{PCL} - 1) \times I_{7.98})$, in which $M_{n,LS}$ was number-average molecular weight of A_mB_n copolymer determined by GPC-MALLS, DP_{PEG} and DP_{PCL} were polymerization degrees of St-PEG and MI-PCL determined by ^{1}H NMR, $M_{n,NMR}$ was molecular weight determined by ^{1}H NMR, and MW_{CTA} was molecular weight of ACP or CPDB.

A_mB_n dendritic comblike copolymers with relatively low polydispersity, multiple disulfide moieties and adjustable segment numbers of A and B grafts are potentially achieved under optimized conditions, in which many factors involving molecular weight of MI-PCL, feed ratio, concentration, temperature and time can play important roles in RAFT SCVP. A couple of copolymerization experiments were performed to reveal their effects on molecular parameters of dendritic copolymers such as molecular weight, CTA functionality and segment numbers of grafted chains (Table 1). For copolymerization using MI-PCL with fixed polymerization degree, both $M_{n,LS}$ and segment numbers of m and n increased with increasing feed ratio of macromonomer to ACP (x), while the corresponding f_{CTA} values were liable to decrease. The extended reaction time generally increased molecular weight of the resultant copolymers due to enhanced monomer conversion and number of branches. By comparing the results as listed in runs 2 and 3 of Table 1, it can be seen that the molecular weight increased from 78 300 (DC2) to 136 000 (DC3) as monomer conversion varied from 35.2% (t = 24 h) to 50.8% (t = 48 h), while the GPC trace of DC3 obtained at a longer time exhibited notably broadened molecular weight distribution although the polydispersity remained low (PDI = 1.21, Figure 4). The gradually broadened distribution with

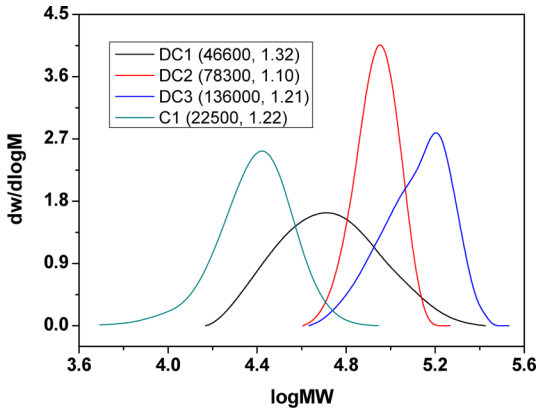

Figure 4. GPC traces (normalized weight distribution) of A_mB_n dendritic comblike copolymers (DC1–DC3) and normal comblike copolymer (C1).

extended time was possibly originated from reduced reactivity of polymer radicals and increased side reactions involving irreversible termination, and the latter was prone to result in partial loss of CTA functionality.[41]

Besides, the effects of monomer concentration and chain length of MI-PCL on the copolymerization were also investigated. The results in various runs using same feed ratio revealed that both total monomer conversion and ACP conversion were remarkably decreased as MI-PCL concentration was reduced from 0.20 (runs 1–3 of Table 1) to 0.05 mol/L (runs 4–8 of Table 1), which could be attributed to reduced rate of radical copolymerization. By comparing the results in runs 4 and 8 of Table 1, it was found that the copolymerization using high-molecular-weight MI-PCL (DP_{NMR} = 43.2) was liable to give DC8 copolymer with lowered CTA functionality and number of grafted chains, suggesting the decreased reactivity of macromonomer with enhanced chain length.

The results as listed in Table 1 indicated that RAFT SCVP could afford dendritic comblike copolymers with intrinsic viscosity in the range of 9.2–26.5 mL/g and average CTA functionality up to 7.5. The similar segment numbers of PEG and PCL grafts in each copolymer revealed the presence of alternating pendent chains. Monomodal distribution was usually noted in GPC traces, and their polydispersity indices were relatively low (PDI = 1.10–1.32, Figure 4), indicating the target dendritic comblike copolymers were successfully obtained by RAFT copolymerization.

Meanwhile, a normal A_mB_n comblike copolymer lack of disulfide linkage (C1, $M_{n,LS}$ = 22 500, PDI = 1.22) was synthesized by RAFT copolymerization of St-PEG and MI-PCL ($M_{n,NMR}$ = 1080) mediated by 2-(2-cyanopropyl) dithiobenzoate (CPDB). C1 copolymer was used as a "linear" analogue

dx.doi.org/10.1021/ma3025283 | Macromolecules 2013, 46, 1325–1336

of dendritic comblike copolymer to investigate the influence of macromolecular architecture on physicochemical properties.

Degradation and Aminolysis of Dendritic Comblike Copolymers. The presence of multiple disulfide moieties in A_mB_n dendritic comblike copolymers enables topological transformations via degradation and coupling.[20] For instance, the cleavage of disulfide functionalities in A_mB_n copolymer upon reductive stimulus such as addition of excess Bu_3P and DTT generates degraded thiol-bearing A_xB_y-type comblike copolymer (a); Multithiol-functionalized $A_mB_n(SH)_o$ copolymer is obtained by aminolysis or reduction of terminal dithiobenzoate moieties, which can be further converted into A_xB_y-type comblike copolymer (b) with at least two thiol functionalities via reduction-triggered degradation (Scheme 2).

Scheme 2. Preparation of Thiol-Functionalized A_mB_n-Type Dendritic Comblike Copolymer ($A_mB_n(SH)_o$) and Degraded A_xB_y-Type Comblike Copolymers (a and b) via Aminolysis and Reduction-Triggered Topological Transformation

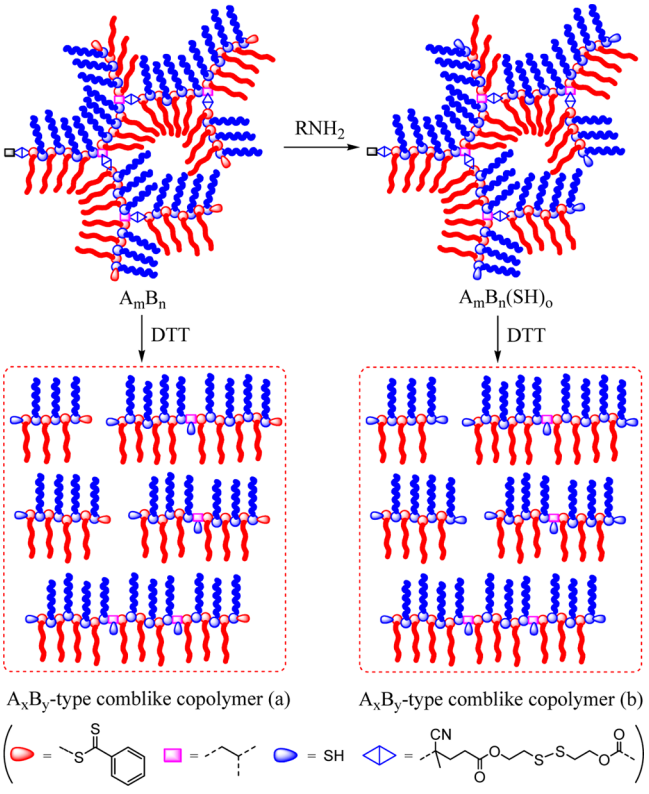

These copolymers can oxidize into high-molecular-weight comblike and dendritic copolymers owing to the high reactivity of thiol moieties. In this study, $(PEG)_m(PCL)_n$ copolymer (DC2, $M_{n,LS}$ = 78300) was chosen as a typical sample to perform cleavage and aminolysis. The reduction using excess Bu_3P afforded degraded $(PEG)_x(PCL)_y$ samples composed of a series of comblike copolymers with different numbers of "branches", evident from significantly decreased molecular weight ($M_{n,LS}$ = 17900) and broadened molecular weight distribution (Figure 5). The gradual degradation upon reductive stimulus also confirmed the branched architecture of dendritic comblike copolymers. Meanwhile, aminolysis of DC2 gave thiol-terminated DC2-SH copolymer ($M_{n,LS}$ = 79600), which was used for drug loading and release as described later.

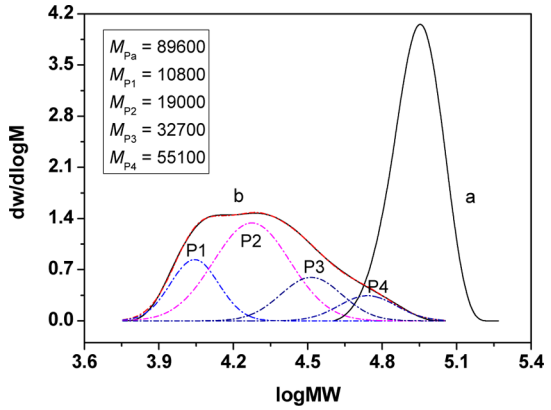

Figure 5. GPC traces (normalized weight distribution) of DC2 copolymer before (a, $M_{n,LS}$ = 78300, PDI = 1.10) and after (b, $M_{n,LS}$ = 17900, PDI = 1.36) treatment with Bu_3P, in which the dash dot line was fitted curve.

Synthesis of $A_mB_nC_o$ Dendritic Toothbrushlike Copolymers. Postpolymerization involving controlled radical polymerization and ring-opening polymerization has a great potential in formation of novel macromolecular architectures. In this study, A_mB_n dendritic comblike copolymers were converted into $A_mB_nC_o$-type dendritic toothbrushlike copolymers as hydrophobic polystyrene (PSt), poly(*tert*-butyl acrylate) (P*t*BA) and poly(methyl methacrylate) (PMMA), and hydrophilic poly(*N*-isopropylacrylamide) (PNIPAM) segments were grown from the "surface" of A_mB_n copolymers via RAFT process.

DC2 ($M_{n,LS}$ = 78300, f_{CTA} = 5.4) was chosen as a typical macro CTA to mediate chain extension polymerization of vinyl monomers (Table 2). In ^{1}H NMR spectra of the isolated $A_mB_nC_o$ copolymers (Figure 6), the characteristic signals of

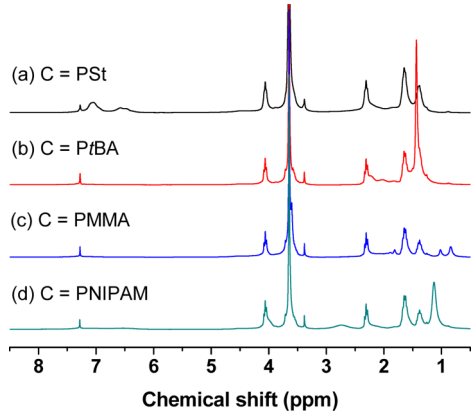

Figure 6. ^{1}H NMR spectra of $(PEG)_m(PCL)_nC_o$ dendritic toothbrushlike copolymers.

each segment were noted at δ 6.2−7.2 (Ph*H* of PSt), 3.60 (CH_3O of PMMA), 2.23 (*CH* of P*t*BA), 1.44 (CH_3 of P*t*BA), 4.01 (*CH* of PNIPAM), 4.06 (CH_2O of PCL), and 3.65 (CH_2CH_2O of PCL), and signals of terminal groups appeared at δ 7.8−8.0 (terminal Ph*H* of PhC(=S)S moieties), 4.6−5.1 (*CHS* of terminal St unit), and about 4.6 (CHS of terminal *t*BA and NIPAM units). The signals at 4.8−5.1 ppm corresponding to *CHS* (terminal comonomer unit) of A_mB_n copolymer completely disappeared, and new signals originating from *CHS* of terminal *t*BA and NIPAM units were almost quantitatively

dx.doi.org/10.1021/ma3025283 | *Macromolecules* 2013, 46, 1325−1336

noted in ^{1}H NMR spectra, revealing that all the dithiobenzoate moieties of A_mB_n copolymer had participated in the RAFT process. Therefore, the average number of C segment was equal to the CTA functionality of A_mB_n copolymer ($o \approx 5.4$). By comparing the integrated peak areas of these protons, $M_{n,NMR}$ values of various copolymers were obtained. Their $M_{n,LS}$ and $M_{n,NMR}$ values were comparable, and both agreed well with theoretical results expected from $M_{n,LS}$ of macro CTA and monomer conversion. The resultant $A_mB_nC_o$ copolymers exhibited roughly symmetric distribution in GPC traces, and their polydispersity indices were in the range of 1.06−1.13 (Figure 7). These results indicated RAFT chain extension

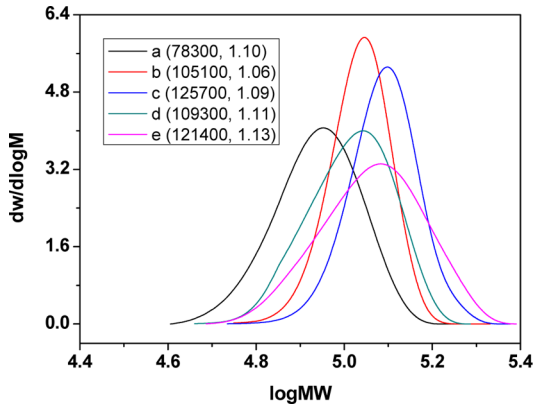

Figure 7. GPC traces (normalized weight distribution) of DC2 (a) and $(PEG)_m(PCL)_nC_o$ (C = PSt (b), P*t*BA (c), PMMA (d), and PNIPAM (e)) copolymers.

polymerization was highly efficiently performed to give $A_mB_nC_o$ dendritic copolymers. The facile synthesis potentially endows the target $A_mB_nC_o$ terpolymers with a wide range of chain length and chemical composition of C segment, and the number of C segment is theoretically equal to f_{CTA} of the macro CTA if all the dithiobenzoate functionalities are activated and side reactions resulting in partial loss of chain radicals are absent.

DSC Analysis of Dendritic Copolymers. DSC measurement was performed to investigate the effects of macromolecular architecture on chain relaxation and melting behaviors (Table S2, Supporting Information). Macromonomers were of melting peaks (T_m) at 29.5 °C (St-PEG), 32.7 and 42.6 °C (MI-PCL), respectively. A_mB_n dendritic comblike copolymer (DC2) had weak glass transitions (T_g) at 47.2 and 54.5 °C and melting range within 15.8−44.9 °C with two melting peaks at 19.0 and 26.8 °C (Figure 8c). Normal A_mB_n comblike copolymer (C1) exhibited obvious glass transitions at 53.6 and 67.3 °C and melting range within 17.8−43.8 °C with melting peak at 33.0 °C (Figure 8d). Besides different chain length of poly(styrene-*alt*-maleimide) backbones, the branching effect could account for their different thermal properties. Although both DC2 and C1 possessed same PEG and PCL side chains, comblike copolymer C1 had longer linear backbone, while dendritic comblike copolymer DC2 was of branched backbones with a couple of comonomer units in each branch, and thus dendritic comblike copolymer could perform the chain relaxation at reduced temperature. Meanwhile, the presence of more compact branched structures in DC2 was liable to form multiple restricted crystalline and noncrystalline regions in which the folding and rearrangement of PEG and PCL chains were more or less disturbed, resulting in

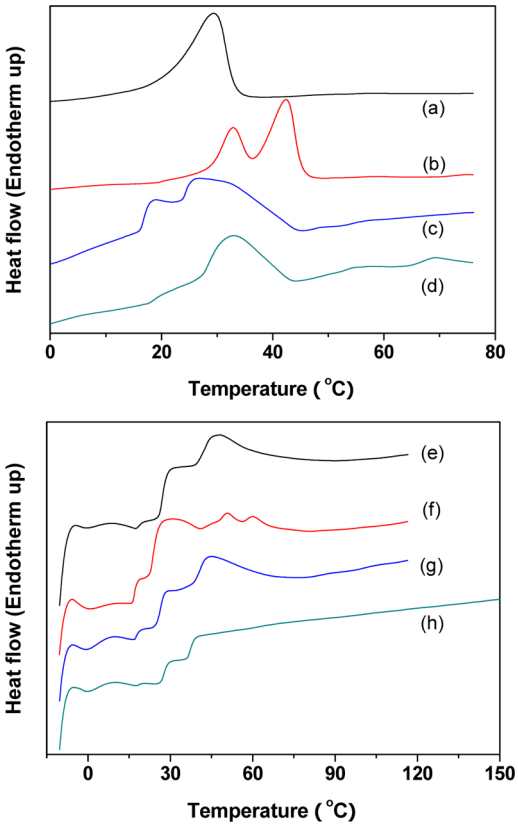

Figure 8. DSC traces of St-PEG (a), MI-PCL (b, DP = 8.2), DC2 (c), C1 (d), and $(PEG)_m(PCL)_nC_o$ copolymers (C = PSt (e), P*t*BA (f), PMMA (g), and PNIPAM (h)).

remarkably reduced melting peaks and broadened melting range in dendritic comblike copolymer.

$A_mB_nC_o$ dendritic toothbrushlike copolymers have more complex chain relaxation and melting processes than A_mB_n dendritic comblike copolymers due to their different architectures. In DSC traces, $(PEG)_m(PCL)_n(PtBA)_o$ showed a notable T_g at 16.9 °C, and other $A_mB_nC_o$ samples only exhibited a relatively weak T_g at about 62.2 (C = PSt), 85.3 (C = PMMA) and 116.1 °C (C = PNIPAM). These observations were in accordance with our previous results,[73−75] in which the T_g values of $(PM)_m$ multiarm star and linear PM with same M_n values decreased in the order linear PM > star-shaped $(PM)_m$ > cleaved PM arm. Interestingly, multiple melting peaks were normally noted in DSC traces of various $A_mB_nC_o$ samples, and the melting range could cover a wide range within 17−75 °C. This phenomenon could be primarily ascribed to the restricted chain movement during crystallization originating from unique architecture of $A_mB_nC_o$ terpolymers. With the introduction of C segments, the resultant dendritic toothbrushlike copolymers possessed a loose out layer comprising C segments and high-density inner layer with overpacking PEG and PCL grafts, and a wide range of microdomains with different types of crystalline and noncrystalline regions and variable degree of crystallinity could be formed, resulting in significantly broadened melting range in DSC traces. The detailed restricted crystallization behaviors of A_mB_n and $A_mB_nC_o$ dendritic copolymers are in progress in our laboratory.

Solution Behavior of Dendritic Copolymers. Parameters involving Mark−Houwink-Sakurada (MHS) exponent (α) and contracting factor (g') can be used to describe different

dx.doi.org/10.1021/ma3025283 | *Macromolecules* 2013, 46, 1325−1336

solution properties between branched polymers and their linear analogues. The MHS exponent of branched polymer is smaller than that of its linear counterpart, and the branching effect can be expressed by the contracting factor defined as the intrinsic viscosity ratio between branched and linear samples with same M_w values.[39−41] Herein we used $[\eta]_{dc}/[\eta]_c$ to illustrate the branching effect, in which $[\eta]_{dc}$ and $[\eta]_c$ were weight-average intrinsic viscosities of dendritic comblike copolymers and normal comblike copolymers with same molecular weights. Three typical A_mB_n (A = PEG, B = PCL) copolymers originating from same macromonomers (DP_{PEG} = 16, DP_{PCL} = 8.2) were subjected to viscosity measurements, and their Mark−Houwink−Sakurada plots over a selected common molecular weight range are listed in Figure 9. The MHS

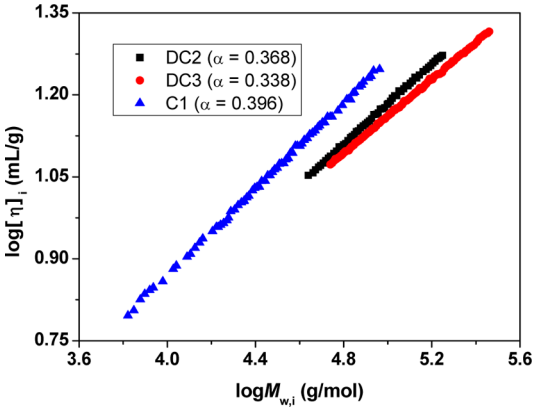

Figure 9. Mark−Houwink−Sakurada plots of normal comblike copolymer (C1) and typical dendritic comblike copolymers (DC2 and DC3).

equations of various copolymers obtained in Table 1 were determined to be $[\eta]_{dc} = 0.221M_w^{0.368}$ (DC2) and $0.296M_w^{0.338}$ (DC 3), and $[\eta]_c = 0.195M_w^{0.395}$ (C1), and the $[\eta]_{dc}/[\eta]_c$ values were calculated to be 0.858 (a) and 0.772 (b). Dendritic comblike copolymer was of reduced α values and smaller intrinsic viscosities than normal comblike copolymer with same molecular weight, further confirming the presence of more compact "hyperbranched" structure in dendritic copolymers.

Dendritic toothbrushlike copolymers may exhibit complex solution properties due to their unique architectures comprising compact "hyperbranched" inner layer and loose "linear" out layer. Mark−Houwink−Sakurada plots of $A_mB_nC_o$ copolymers (Figure 10b−e) gave α values in the range of 0.484−0.552, and the MHS equations of various copolymers were determined to be $[\eta] = 0.0327M_w^{0.552}$ (b, *C* = PSt), $0.0697M_w^{0.498}$ (c, *C* = P*t*BA), $0.0692M_w^{0.484}$ (d, *C* = PMMA) and $0.0598M_w^{0.506}$ (e, *C* = PNIPAM). As compared with the MHS equations of linear polymers $[\eta]_l = 0.0129M_w^{0.740}$ (PSt), $0.0225M_w^{0.659}$ (P*t*BA) and $0.0135M_w^{0.686}$ (PMMA),[41] the MHS exponent and intrinsic viscosity values of different samples with same M_w values were found to decrease in the order linear C segment > $A_mB_nC_o$ dendritic toothbrush copolymer > A_mB_n dendritic comblike copolymer. These results revealed that the introduction of C segments into the surface of dendritic comblike copolymer could partly decrease the compact degree of dendritic macromolecules.

DOX-Loading and Release from A_mB_n Copolymer Aggregates. Aqueous self-assembly of C1, DC2, and DC2-SH was performed to prepare blank and DOX-loaded

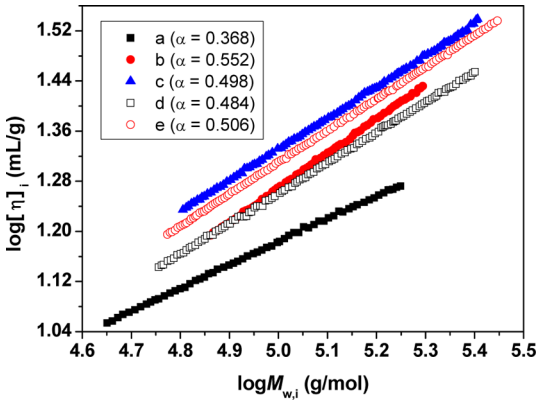

Figure 10. Mark−Houwink-Sakurada plots of DC2 (a) and $(PEG)_m(PCL)_nC_o$ copolymers (*C* = PSt (b), P*t*BA (c), PMMA (d), and PNIPAM (e)).

copolymer aggregates. DLS results revealed that various copolymers were liable to self-assemble into aggregates with bimodal distribution. DC2 formed blank aggregates with peak diameters (D_{peak}) of 22.8 and 178.1 nm, and its DOX-loaded copolymer aggregates had D_{peak} values of 18.7 and 232.3 nm (Figure 11a). Although DC2-SH formed bimodal-distributed

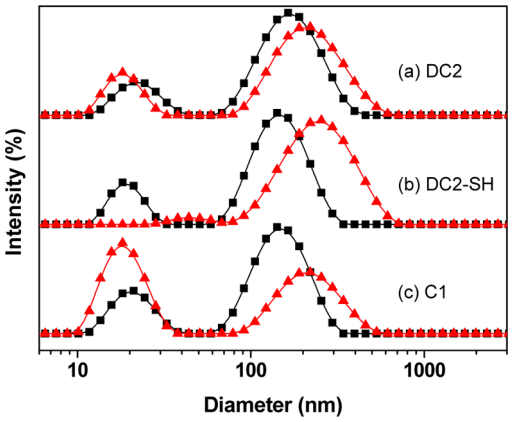

Figure 11. DLS plots of blank (square) and DOX-loaded (triangle, $W_{polymer}$:W_{DOX} = 5:1) copolymer aggregates (*c* = 0.5 mg/mL) in PBS solution (pH 7.4, 50 mM) at 37 °C.

aggregates (D_{peak} = 19.5 and 153.4 nm), its DOX-incorporated aggregates exhibited a predominant distribution (D_{peak} = 263.3 nm) besides a very small peak centering at 45.5 nm (Figure 11b), which revealed the addition of hydrophobic drug could optimize the self-assembly process. Similarly, bimodal distribution was noted in DLS plots of C1 aggregates. These results indicated self-assembly behaviors were affected by a combination of macromolecular architecture, molecular weight, end group and even added drugs.

Owing to the change in macromolecular architecture and intermolecular interactions, the presence of cleavable disulfide moieties in dendritic comblike copolymers was liable to damage the self-assembled structures upon reductive stimulus. In TEM images of blank DC2 aggregates (Figure S5a, Supporting Information), both unimolecular micelles ($D \approx 5.0$ nm) and conventional micelles ($D \approx 60$ nm) were observed, and the particle sizes were reasonably smaller than those estimated by DLS. With addition of 10 mM DTT, nanoparticles corresponding to unimolecular micelles and aggregates formed

dx.doi.org/10.1021/ma3025283 | *Macromolecules* 2013, 46, 1325−1336

Table 3. Influence of Architecture and Compositions on Properties of Copolymer Aggregates

copolymer	D (nm)[a]	PD[a]	D_{peak} (nm)[a]	D (nm)[b]	PD[b]	D_{peak} (nm)[b]	DLC (%)[c]	DLE (%)[c]
DC2	87.4	0.585	22.8, 178.1	93.3	0.650	18.7, 232.3	3.32	16.6
DC2-SH	90.8	0.570	19.5, 153.4	190.8	0.210	45.5, 263.3	2.97	14.9
C1	100.3	0.387	21.3, 154.5	36.1	0.527	19.0, 227.8	3.46	17.3

[a]Cumulant diameter (D), particle size distribution (PD), and peak diameter (D_{peak}) of blank copolymer aggregates obtained by DLS analyses. [b]Various parameters of DOX-loaded copolymer aggregates (5:1). [c]Determined by fluorescence analysis.

by a couple of copolymers were formed (Figure S5b, Supporting Information). The remarkably decreased particle size could be attributed to reduction-triggered destabilization and rearrangement of copolymer aggregates originating from the end group effect, decreased molecular weight, and weakened intermolecular interactions.[76−83]

DOX loading and release properties of A_mB_n and $A_mB_n(SH)_o$ copolymers were investigated to better understand the potential of copolymer aggregates. The drug loading capacity (DLC) and drug loading efficiency (DLE) of copolymer aggregates were determined by fluorescence analysis (Table 3). The DLE value of DC2 aggregates (DLE = 16.6%) was comparable to that of C1 aggregates (DLE = 17.3%), and both were slightly higher than that of DC2-SH aggregates (DLE = 14.9%). The in vitro drug release of DOX from the copolymer aggregates was performed in PBS solution (pH 7.4, 50 mM) at 37 °C. The release rate was liable to decrease in the order DC2-SH > C1 > DC2 (Figure 12), revealing both macromolecular architecture

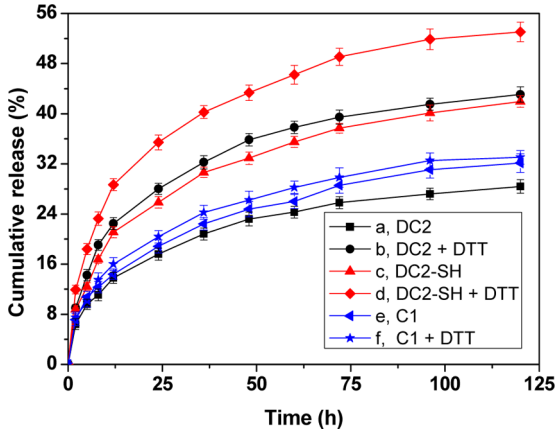

Figure 12. In vitro drug release profiles of DOX-loaded copolymer aggregates in PBS solution (pH 7.4, 50 mM) at 37 °C with or without addition of 10 mM DTT.

and end group could play important roles in drug release kinetics. As expected, the cumulative release from DOX-loaded C1 aggregates in the presence of 10 mM DTT was only slightly higher than that without DTT, while a faster release from the dendritic copolymer aggregates upon reductive stimulus was noted. After 120 h, about 28.4% (DC2), 43.1% (DC2 + DTT), 42.0% (DC2-SH), 53.1% (DC2-SH + DTT), 32.1% (C1), and 33.0% (C1 + DTT) of encapsulated DOX could be efficiently released from the DOX-loaded copolymer aggregates, and no burst release behaviors were noted in all cases. These results indicated the DOX release kinetics was accelerated by the introduction of reductive stimulus and terminal thiol functionality, which could be ascribed to dynamic destabilization of copolymer aggregates resulting from the change in molecular weight and end group.[76−83] The addition of excess DTT led to the gradual cleavage of disulfide moiety to form thiol-terminated degraded comblike copolymers, and the change in microenvironment could induce rearrangement and reaggregation of copolymers due to variable inter and intramolecular interactions, and thus the encapsulated DOX could be faster released. With variation of end group and addition of reductive stimulus, the drug release kinetics could be tuned in a wide range, revealing the great potential of dendritic comblike copolymer aggregates for biomedical application.

CONCLUSION

We have demonstrated that the combination of RAFT SCVP and sequence-controlled copolymerization could be efficiently used to construct novel multicleavable amphiphilic dendritic copolymers via one or two step reactions. RAFT copolymerization of St-PEG and MI-PCL in the presence of ACP afforded $(PEG)_m(PCL)_n$ dendritic comblike copolymers with alternating PEG and PCL pendent chains and multiple disulfide functionalities in branching points, and $A_mB_nC_o$ dendritic toothbrushlike copolymers were generated by a subsequent chain extension polymerization of vinyl monomers. The resultant $(PEG)_m(PCL)_n$ dendritic comblike copolymers had adjustable molecular weight, relatively low polydispersity, similar numbers of PEG and PCL grafts, and variable CTA functionality, evident from ^{1}H NMR and GPC-MALLS analyses. Reduction-triggered degradation, viscosity measurement and DSC results fully confirmed the branched architectures of various dendritic copolymers. In vitro drug release revealed the disulfide-linked copolymer aggregates could rapidly release the encapsulated doxorubicin when triggered by 10 mM DTT, and the drug release kinetics was remarkably affected by macromolecular architecture, end group and reductive stimulus. These reduction-sensitive and biodegradable dendritic copolymer aggregates had a great potential for biomedical applications. Moreover, the general methodology can be extended to facile synthesis of numerous dendritic copolymers with rich chemical composition, tunable segment length and versatile stimuli-responsive functionality.

ASSOCIATED CONTENT

Supporting Information

Synthetic routes to St-PEG and MI-PCL macromonomers, synthesis and DSC data, ^{1}H and ^{13}C NMR spectra of ACP, HTD, and macromonomers, IR spectra of ACP and various polymers, and TEM images of DC2 copolymer aggregates. This material is available free of charge via the Internet at http://pubs.acs.org.

AUTHOR INFORMATION

Corresponding Author

*E-mail: ylzhao@suda.edu.cn.

Author Contributions

†These authors contributed equally to this work.

Notes

The authors declare no competing financial interest.

■ ACKNOWLEDGMENTS

This work was financially supported by the National Natural Science Foundation of China (Grants 20874067, 21074081 and 21274096), the Key Project of Chinese Ministry of Education (No. 209049), and the Project Funded by the Priority Academic Program Development of Jiangsu Higher Education Institutions. The authors are grateful for helpful discussions from Jianzhong Du at Tongji University.

■ REFERENCES

(1) Harth, E. M.; Hecht, S.; Helms, B.; Malmstrom, E. E.; Fréchet, J. M. J.; Hawker, C. J. *J. Am. Chem. Soc.* **2002**, *124*, 3926−3938.
(2) Gillies, E. R.; Jonsson, T. B.; Fréchet, J. M. J. *J. Am. Chem. Soc.* **2004**, *126*, 11936−11943.
(3) Gao, C.; Yan, D. Y. *Prog. Polym. Sci.* **2004**, *29*, 183−275.
(4) Jin, H. B.; Huang, W.; Zhu, X. Y.; Zhou, Y. F.; Yan, D. Y. *Chem. Soc. Rev.* **2012**, *41*, 5986−5997.
(5) Voit, B. I.; Lederer, A. *Chem. Rev.* **2009**, *109*, 5924−5973.
(6) Wurm, F.; Frey, H. *Prog. Polym. Sci.* **2011**, *36*, 1−52.
(7) Carlmark, A.; Hawker, C. J.; Hult, A.; Malkoch, M. *Chem. Soc. Rev.* **2009**, *38*, 352−362.
(8) Zagar, E.; Zigon, M. *Prog. Polym. Sci.* **2011**, *36*, 53−88.
(9) Konkolewicz, D.; Monteiro, M. J.; Perrier, S. *Macromolecules* **2011**, *44*, 7067−7087.
(10) Khandare, J.; Calderon, M.; Dagia, N. M.; Haag, R. *Chem. Soc. Rev.* **2012**, *41*, 2824−2848.
(11) Li, Z. B.; Kesselman, E.; Talmon, Y.; Hillmyer, M. A.; Lodge, T. P. *Science* **2004**, *306*, 98−101.
(12) Lodge, T. P.; Rasdal, A.; Li, Z. B.; Hillmyer, M. A. *J. Am. Chem. Soc.* **2005**, *127*, 17608−17609.
(13) Moughton, A. O.; Hillmyer, M. A.; Lodge, T. P. *Macromolecules* **2012**, *45*, 2−19.
(14) Fukae, K.; Terashima, T.; Sawamoto, M. *Macromolecules* **2012**, *45*, 3377−3386.
(15) Gao, H. F.; Matyjaszewski, K. *Prog. Polym. Sci.* **2009**, *34*, 317−350.
(16) Altintas, O.; Vogt, A. P.; Barner-Kowollik, C.; Tunca, U. *Polym. Chem.* **2012**, *3*, 34−45.
(17) Bapat, A. P.; Roy, D.; Ray, J. G.; Savin, D. A.; Sumerlin, B. S. *J. Am. Chem. Soc.* **2011**, *133*, 19832−19838.
(18) Syrett, J. A.; Haddleton, D. M.; Whittaker, M. R.; Davis, T. P.; Boyer, C. *Chem. Commun.* **2011**, *47*, 1449−1451.
(19) Zhang, Q.; Li, G. Z.; Becer, C. R.; Haddleton, D. M. *Chem. Commun.* **2012**, *48*, 8063−8065.
(20) Jiang, X.; Zhang, M. J.; Li, S. X.; Shao, W.; Zhao, Y. L. *Chem. Commun.* **2012**, *48*, 9906−9908.
(21) Ye, C. N.; Zhao, G. D.; Zhang, M. J.; Du, J. Z.; Zhao, Y. L. *Macromolecules* **2012**, *45*, 7429−7439.
(22) Sheiko, S. S.; Sumerlin, B. S.; Matyjaszewski, K. *Prog. Polym. Sci.* **2008**, *33*, 759−785.
(23) Lee, H. I.; Pietrasik, J.; Sheiko, S. S.; Matyjaszewski, K. *Prog. Polym. Sci.* **2010**, *35*, 24−44.
(24) Iha, R. K.; Wooley, K. L.; Nyström, A. M.; Burke, D. J.; Kade, M. J.; Hawker, C. J. *Chem. Rev.* **2009**, *109*, 5620−5686.
(25) Xia, Y.; Boydston, A. J.; Grubbs, R. H. *Angew. Chem., Int. Ed.* **2011**, *50*, 5882−5885.
(26) Xia, Y.; Li, Y. J.; Burts, A. O.; Ottaviani, M. F.; Tirrell, D. A.; Johnson, J. A.; Turro, N. J.; Grubbs, R. H. *J. Am. Chem. Soc.* **2011**, *133*, 19953−19959.
(27) Feng, C.; Li, Y. J.; Yang, D.; Hu, J. H.; Zhang, X. H.; Huang, X. Y. *Chem. Soc. Rev.* **2011**, *40*, 1282−1295.
(28) Li, A.; Li, Z.; Zhang, S. Y.; Sun, G. R.; Policarpio, D. M.; Wooley, K. L. *ACS Macro Lett.* **2012**, *1*, 241−245.
(29) Xu, Y. Y.; Bolisetty, S.; Ballauff, M.; Müller, A. H. E. *J. Am. Chem. Soc.* **2009**, *131*, 1640−1641.
(30) Chen, Y. M. *Macromolecules* **2012**, *45*, 2619−2631.
(31) Fréchet, J. M. J.; Henmi, M.; Gitsov, I.; Aoshima, S.; Leduc, M. R.; Grubbs, R. B. *Science* **1995**, *269*, 1080−1083.
(32) Matyjaszewski, K. *Macromolecules* **2012**, *45*, 4015−4039.
(33) Rikkou-Kalourkoti, M.; Matyjaszewski, K.; Patrickios, C. S. *Macromolecules* **2012**, *45*, 1313−1320.
(34) Pugh, C.; Singh, A.; Samuel, R.; Ramos, K. M. B. *Macromolecules* **2010**, *43*, 5222−5232.
(35) Muthukrishnan, S.; Jutz, G.; André, X.; Mori, H.; Müller, A. H. E. *Macromolecules* **2005**, *38*, 9−18.
(36) Powell, K. T.; Cheng, C.; Wooley, K. L. *Macromolecules* **2007**, *40*, 4509−4515.
(37) Chiefari, J.; Chong, Y. K.; Ercole, F.; Krstina, J.; Jeffery, J.; Le, T. P. T.; Mayadunne, R. T. A.; Meijs, G. F.; Moad, C. L.; Moad, G.; Rizzardo, E.; Thang, S. H. *Macromolecules* **1998**, *31*, 5559−5562.
(38) Wan, W. M.; Pan, C. Y. *Macromolecules* **2008**, *41*, 5085−5088.
(39) Wang, Z. M.; He, J. P.; Tao, Y. F.; Yang, L.; Jiang, H. J.; Yang, Y. L. *Macromolecules* **2003**, *36*, 7446−7452.
(40) Vogt, A. P.; Sumerlin, B. S. *Macromolecules* **2008**, *41*, 7368−7373.
(41) Zhang, C. B.; Zhou, Y.; Liu, Q.; Li, S. X.; Perrier, S.; Zhao, Y. L. *Macromolecules* **2011**, *44*, 2034−2049.
(42) Zhang, M. J.; Liu, H. H.; Shao, W.; Ye, C. N.; Zhao, Y. L. *Macromolecules* **2012**, *45*, 9312−9325.
(43) Han, J.; Li, S. P.; Tang, A. J.; Gao, C. *Macromolecules* **2012**, *45*, 4966−4977.
(44) Ida, S.; Terashima, T.; Ouchi, M.; Sawamoto, M. *J. Am. Chem. Soc.* **2009**, *131*, 10808−10809.
(45) Ida, S.; Ouchi, M.; Sawamoto, M. *J. Am. Chem. Soc.* **2010**, *132*, 14748−14750.
(46) Hibi, Y.; Ouchi, M.; Sawamoto, M. *Angew. Chem., Int. Ed.* **2011**, *50*, 7434−7437.
(47) Nakatani, K.; Ogura, Y.; Koda, Y.; Terashima, T.; Sawamoto, M. *J. Am. Chem. Soc.* **2012**, *134*, 4373−4383.
(48) Satoh, K.; Saitoh, S.; Kamigaito, M. *J. Am. Chem. Soc.* **2007**, *129*, 9586−9587.
(49) Mizutani, M.; Satoh, K.; Kamigaito, M. *J. Am. Chem. Soc.* **2010**, *132*, 7498−7507.
(50) Satoh, K.; Matsuda, M.; Nagai, K.; Kamigaito, M. *J. Am. Chem. Soc.* **2010**, *132*, 10003−10005.
(51) Li, Z. L.; Li, L.; Deng, X. X.; Zhang, J. J.; Dong, B. T.; Du, F, S.; Li, Z. C. *Macromolecules* **2012**, *45*, 4590−4598.
(52) Chen, G. Q.; Wu, Z. Q.; Wu, J. R.; Li, Z. C.; Li, F. M. *Macromolecules* **2000**, *33*, 232−234.
(53) Pfeifer, S.; Lutz, J.-F. *J. Am. Chem. Soc.* **2007**, *129*, 9542−9543.
(54) Badi, N.; Lutz, J.-F. *Chem. Soc. Rev.* **2009**, *38*, 3383−3390.
(55) Berthet, M.-A.; Zarafshani, Z.; Pfeifer, S.; Lutz, J.-F. *Macromolecules* **2010**, *43*, 44−50.
(56) Lutz, J.-F.; Schmidt, B. V. K. J.; Pfeifer, S. *Macromol. Rapid Commun.* **2011**, *32*, 127−135.
(57) Chan-Seng, D.; Zamfir, M.; Lutz, J.-F. *Angew. Chem., Int. Ed.* **2012**, *51*, 12254−12257.
(58) Moughton, A. O.; Sagawa, T.; Gramlich, W. M.; Seo, M.; Lodge, T. P.; Hillmyer, M. A. *Polym. Chem.* **2013**, *4*, 166−173.
(59) Zhu, H.; Deng, G. H.; Chen, Y. M. *Polymer* **2008**, *49*, 405−411.
(60) Deng, G. H.; Chen, Y. M. *J. Polym. Sci., Part A: Polym. Chem.* **2009**, *47*, 5527−5533.
(61) Xia, N.; Zhang, G. L.; Li, T.; Wang, W.; Zhu, H.; Chen, Y. M.; Deng, G. H. *Polymer* **2011**, *52*, 4581−4589.
(62) Li, S. X.; Ye, C. N.; Zhao, G. D.; Zhang, M. J.; Zhao, Y. L. *J. Polym. Sci., Part A: Polym. Chem.* **2012**, *50*, 3135−3148.
(63) Zhao, Y. L.; Jiang, J.; Liu, H. W.; Chen, C. F.; Xi, F. *J. Polym. Sci., Part A: Polym. Chem.* **2001**, *39*, 3960−3966.
(64) Zhao, Y. L.; Zhang, J. M.; Jiang, J.; Chen, C. F.; Xi, F. *J. Polym. Sci., Part A: Polym. Chem.* **2002**, *40*, 3360−3366.
(65) Zhao, Y. L.; Chen, C. F.; Xi, F. *J. Polym. Sci., Part A: Polym. Chem.* **2003**, *41*, 2156−2165.
(66) Deng, G. H.; Chen, Y. M. *Macromolecules* **2004**, *37*, 18−26.

(67) Liu, Q. C.; Chen, Y. M. *Macromol. Chem. Phys.* **2007**, *208*, 2455−2462.
(68) Konkolewicz, D.; Gray-Weale, A.; Perrier, S. *J. Am. Chem. Soc.* **2009**, *131*, 18075−18077.
(69) Konkolewicz, D.; Poon, C. K.; Gray-Weale, A.; Perrier, S. *Chem. Commun.* **2011**, *47*, 239−241.
(70) Mantovani, G.; Lecolley, F.; Tao, L.; Haddleton, D. M.; Clerx, J.; Cornelissen, J. J. L. M.; Velonia, K. *J. Am. Chem. Soc.* **2005**, *127*, 2966−2973.
(71) Mitsukami, Y.; Donovan, M. S.; Lowe, A. B.; McCormick, C. L. *Macromolecules* **2001**, *34*, 2248−2256.
(72) Tao, L.; Liu, J. Q.; Tan, B. H.; Davis, T. P. *Macromolecules* **2009**, *42*, 4960−4962.
(73) Zhao, Y. L.; Cai, Q.; Jiang, J.; Shuai, X. T.; Bei, J. Z.; Chen, C. F.; Xi, F. *Polymer* **2002**, *43*, 5819−5825.
(74) Zhao, Y. L.; Shuai, X. T.; Chen, C. F.; Xi, F. *Chem. Mater.* **2003**, *15*, 2836−2843.
(75) Zhao, Y. L.; Chen, Y. M.; Chen, C. F.; Xi, F. *Polymer* **2005**, *46*, 5808−5819.
(76) Kujawa, P.; Watanabe, H.; Tanaka, F.; Winnik, F. M. *Eur. Phys. J. E.* **2005**, *17*, 129−137.
(77) Koga, T.; Tanaka, F.; Motokawa, R.; Koizumi, S.; Winnik, F. M. *Macromolecules* **2008**, *41*, 9413−9422.
(78) Xu, J.; Tao, L.; Boyer, C.; Lowe, A. B.; Davies, T. P. *Macromolecules* **2011**, *44*, 299−312.
(79) Du, J. Z.; Willcock, H.; Patterson, J. P.; Portman, I.; O'Reilly, R. K. *Small* **2011**, *7*, 2070−2080.
(80) Zhu, Y. Q.; Liu, L.; Du, J. Z. *Macromolecules* **2013**, *46*, 194−203.
(81) Klaikherd, A.; Nagamani, C.; Thayumanavan, S. *J. Am. Chem. Soc.* **2009**, *131*, 4830−4838.
(82) Meng, F. H.; Hennink, W. E.; Zhong, Z. Y. *Biomaterials* **2009**, *30*, 2180−2198.
(83) Khorsand Sourkohi, B.; Schmidt, R.; Oh, J. K. *Macromol. Rapid Commun.* **2011**, *32*, 1652−1657.